SPALL FRACTURE OF METALLIC CIRCULAR PLATES, VESSEL ENDPLATES AND CONICAL FRUSTUMS DRIVEN BY DIRECT EXPLOSIVE LOADS

T. Hiroe, K. Fujiwara, H. Hata, and D. Tsutsumi

Department of Mechanical System Engineering, Kumamoto University, Kumamoto 860-8555, Japan

Abstract. Dynamic fracture experiments are conducted for circular plates, vessel endplates and conical frustums of A2017-7075 aluminum alloys and 304 stainless steel, using a testing apparatus developed applying wire-row explosion technique to initiation, where tensile stress waves are generated producing spall in the specimens by the direct incidence of plane detonation waves of the explosive PETN. A VISAR system is adopted to observe the free-surface velocity histories of the specimens. The signals for basic circular plate specimens indicate the characteristics of the failure for tested materials, effects of explosive thickness variations and the configuration of specimens. Hydro codes are satisfactorily applied to simulate the experimental signal data and observed damage phenomena of recovered specimens. Next, an explosive-filled cylindrical vessel with an endplate at the one end is initiated at the other end surface and expanded by axially propagating explosive detonation to fracture. Both the VISAR signals and numerical simulation indicate a pullback signal of spallation at the endplate. Finally conic frustums are also loaded by plane detonation, showing different type of spall failure due to the additional reflected waves from the slopping side surfaces.

Keywords: Spall fracture, explosive, wire explosion, frustum, endplate, axial crack.
PACS: 62.20.Mk, 62.50+p.

INTRODUCTION

Spallation driven by direct explosive loadings [1] occurs due to tensile stresses generated by the interaction of expansion waves emerged due to the reflection of strong shock waves at the free surfaces of the structural components and other strong expansion waves coming from behind the detonation waves. Previously, authors had developed explosive loading devices producing planar detonation waves in powder pentaerythritol-tetranitrate (PETN) with the use of exploding wire initiation, showing some applications to spall tests of circular plates [2] and expansion of cylinders [3]. In this paper, spallation behavior driven by direct explosive loads has been investigated for three types of specimens: circular plates, conical frustums and vessel endplates of aluminum alloys and stainless steel with variations of specimen configurations and explosive heights. The characteristics of three types of specimens are introduced comparing observation of free-surface velocities and damages with numerical simulations.

EXPERIMENTAL NUMERICAL PROCEDURE

Experiments are performed utilizing the explosion test facilities at the Shock Wave and Condensed Matter Research Center, Kumamoto University. Two kinds of explosive assemblies were developed for spall tests. The one is for circular plates and conical frustums, where slab-like installed powder PETN (0.92-0.98g/cc) is initiated by the simultaneous explosion of parallel

TABLE 1. Summary of spall test conditions

| Specimen types | Materials | Plate configurations | | PETN thickness, |
		Plate thickness, mm	Top/bottom dia.**, mm	mm
Circular plate	A2017	20	50/50	15
	A2024	20	ditto	10, 15, 20
	A7075	2, 5, 10, 20	ditto	ditto
	SUS304	20	ditto	ditto
Conical frastum	A2017	20	30/50, 24/50, 12/50	15
	SUS304	20	ditto	20
Vessel endplate*	SUS304	6	50/50	100

*SUS304 cylinder sizes: $34\phi \times 3t \times 100L(mm)$, **Sloping angles: 26.5, 33.0, 43.5 deg. for 30/50, 24/50, 12/50
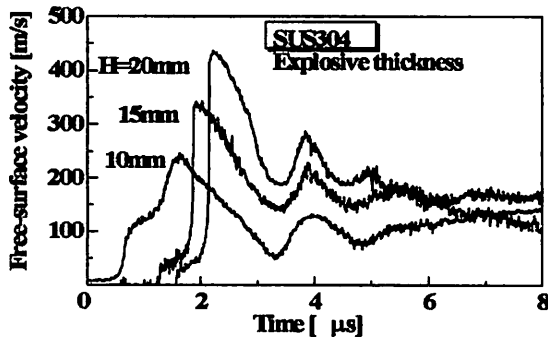
a. Explosive thickness effect
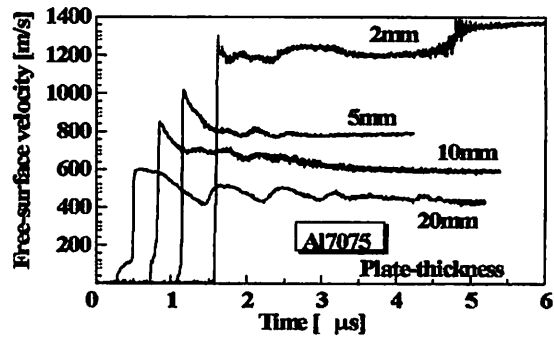
b. Plate thickness effect

c. Endplate of model vessel

Figure 1. Typical VISAR signals for circular plate specimens, showing the effects of a. explosive thicknesses for SUS304 (20mm thickness), b. plate thicknesses for A7075 with explosive height of 10mm and c. endplate of model vessel of SUS304.
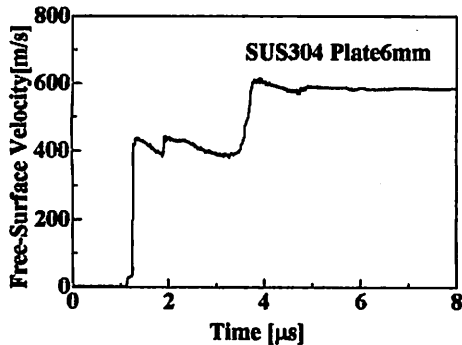
copper wire rows (diameter: 175μm, the ratio of PETN thickness of wire interval: 1.3-1.5) placed over the entire outer surface using an impulsive discharge current from a capacitor bank of 40μF, 20kV, producing a planar detonation front in the PETN layer immediately after the initial explosion and transferring a one-dimensional triangular pressure pulse to the specimen., and the second is for an endplate welded to a cylinder vessel, where

PETN column fully installed in the vessel is also initiated by the wire-row explosion at the other end-surface, producing an axially-propagating expanding detonation wave. These three types of specimens were machined from plates and a tubular cylinder of three aluminum alloys of T4 heat, JIS series: A2017, A2024, A7075 and an 18Cr-8Ni stainless steel, JIS SUS304. All the test conditions: thicknesses of explosives and plates

for circular specimens, diameter ratios of top and bottom surfaces for frustums with constant height, the configurations of the vessel with the endplate are summarized in Table 1. The damages of the specimens were monitored by measuring time-histories of free surface velocity with use of a laser interferometry system VISAR, ATA model 605, and observed in the cross-sections of recovered specimens for all the cases. The expansion behavior of the model vessel was recorded with a high speed camera: IMACON 468. Numerical simulations were performed for all the experiments using a hydro code: Autodyn 2D.

EXPERIMENTAL SPALL BEHAVIOR AND FREE SURFACE VELOCITIES

Figure 1 shows typical VISAR records for circular plate specimens and a model vessel. The signals for SUS304 plates with 20mm thickness in Fig. 1a indicate the obvious effect of PETN height H on the peak stress attenuation or release waves coming from the inner surface of the explosive during the transmission of shock waves across the specimens. These signals also recommend the concept of effective PETN thickness in numerical

simulations, taking the initial interference process before stable detonation into consideration. Such amplitudes of peak velocity are roughly predicted from the Hugoniot curves for the materials and the wave patterns are basically same, that is, the surface velocity rises abruptly after the initial elastic precursor and drops immediately without duration. The standard spall parameters for the materials were calculated, which are close to the reference data [4]. In Fig. 1b for an endplate of the model vessel, it is recognized that a pullback signal has emerged instantly after the initial increase of the free-surface velocity. Other records for specimen thickness effect of A2017 indicated that the smaller pullback signals or tensile stresses are generated in the thinner plates, and finally explicit spall fracture is not observed for the plate thickness of 2 mm. The records for frustums showed rather obscure damage signals with complex and irregular waves. Figure 2 represents framing records for the vessel specimen, showing axially phased expansion is propagating symmetrical to the endplate. The fracture at the welded joint of a cylinder and an endplate occurs at rather early time, and finally the endplate expands spherically. Figure 3 shows typical photos of spall damages in cross-sections

a. 30μs   b. 40μs   c. 50μs
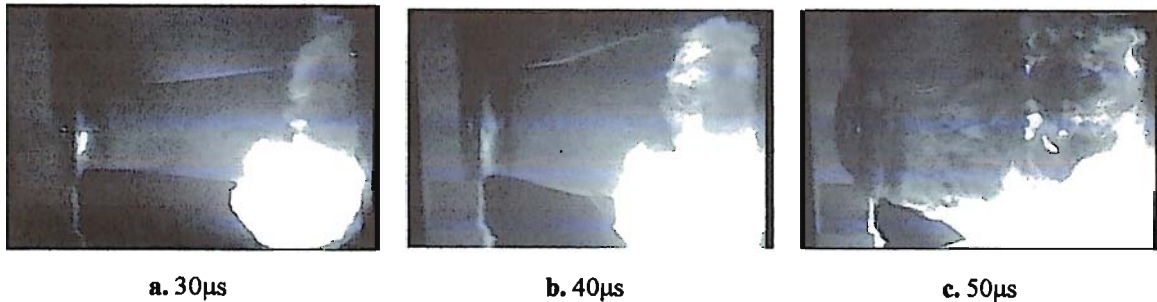
Figure 3. Framing records for exploding model vessel with a endplate

a. Circular plate   b. Conical frustum
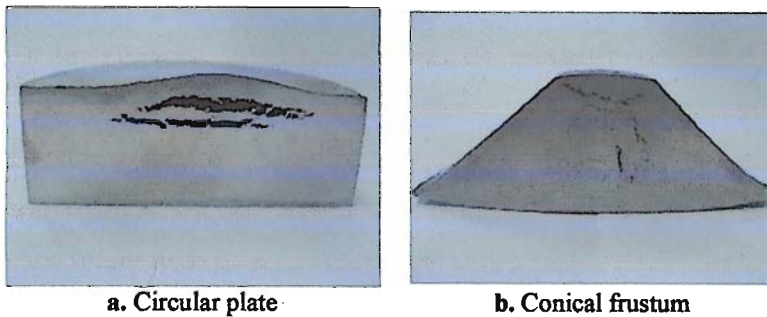
Figure 4. Cross sectional photos of recovered a. circular plate (50/50mm) and b. conical frustum (12/50mm, slopping 43.5 deg.) of SUS304 with PETN height of 20mm

for recovered circular plate and conical frustum (12/50mm) of SUS304 (PETN: 20mm). Such spall-layer thickness as shown in Fig. 3a corresponds with the observed wave length of the VISAR signal in Fig. 1a, but Fig. 3b indicates rather unique spallation showing additional axial cracks with a usual spall crack parallel to the top surface. Such axial cracks became dominant as increase of slopping angle, and for A2017 frustums more destructive damages were observed due to less strength. In case of the endplate, obvious cracks were not observed in the cross-section due to the following large spherical deformation after the spallation.

NUMERICAL SIMULATION AND DISCUSSION

Numerical simulation almost reproduced the VISAR signals and the exploding model vessel s. Figure 4 shows typical numerical damage distributions based on stress criterion for three types of specimens: a circular plate and a conical frustum of A2017 after stress disappearance and a vessel with an endplate of SUS304 just after the spallation. Numerical damages in Fig. 4 emphatically depict experimental damages in Fig. 3 well in spite of different materials. Numerical time-histories of stress distributions in the conical

frustum indicated three rarefaction waves: the ones reflected back at the top and slopping free surfaces and another ones coming from the inner surface of the explosive interact one another, producing spalling failure in the specimens. In Fig. 4c, obvious spallation is generated in the endplate just after the reflection of triangular-shaped pressure pulse with rather long tail at the surface and before the following deformation, and this phenomenon coincided with the VISAR signal in Fig. 1b.

REFERENCES

1. Tuler, F. and Butcher, B. M., "Criterion for the Time Dependence of Dynamic Fracture", *Int. J. Fract. Mech*, Vol. 4, 1968, pp.431-437.
2. Hiroe, T., Fujiwara, K., Hideo Matsuo, and Thadhani, N. N., "Explosively Produced Spalling in Metals and Its Loading Effects", Proc. of the 4th International Symposium on *Impact Engineering*, 16-18 July, Kumamoto, Japan, 2001, 851-856.
3. Hiroe, T., Fujiwara, K., Abe, T., and Yoshida, M., "Rapid Expansion and Fracture of Metallic Cylinders Driven by Explosive Loads", Proc. of 13th Biennial International Conference of the APS Topical Group on *Shock Compression of Condensed Matter*, July 20-25, Portland OR, 2003, 465–472
4. Steinberg, D. J., "Equation of State and Strength Properties of Selected Materials", *LLNL Report UCRL-MA-106439*, 1991.

a. Circular plate (A2017)

b. Conical frustum (A2017)

c. Vessel endplate (SUS304)
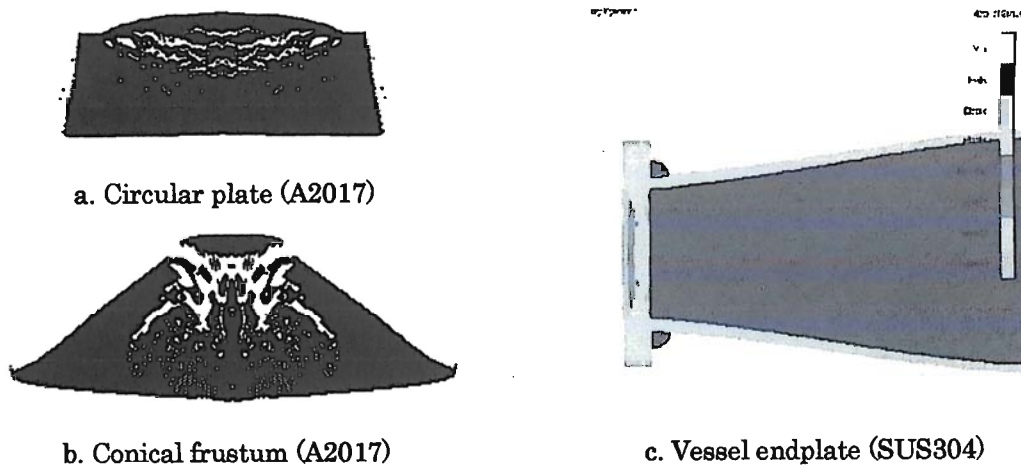
Figure 5. Typical numerical damage distributions based on stress criterion for a. circular plate (A2017), b. conical frustum of 12/50mm (A2017) and c. vessel endplate (SUS304) at 23.5 □s just after the spallation has been generated.